UCRL-JC-122501
PREPRINT
CONF-951182--6

Simulation of Experimentally Achieved Detached Plasmas Using the UEDGE Code

G.D. Porter, S. Allen, M. Fenstermacher, D. Hill, R. Jong, T. Leonard, D. Nilson, M. Rensink, T. Rognlien, G. Smith and the entire DIII-D team

This paper was prepared for submittal to the
American Physical Society, Division of Plasma Physics
37th Annual Meeting
Louisville, KY
November 6-10, 1995

October 30, 1995

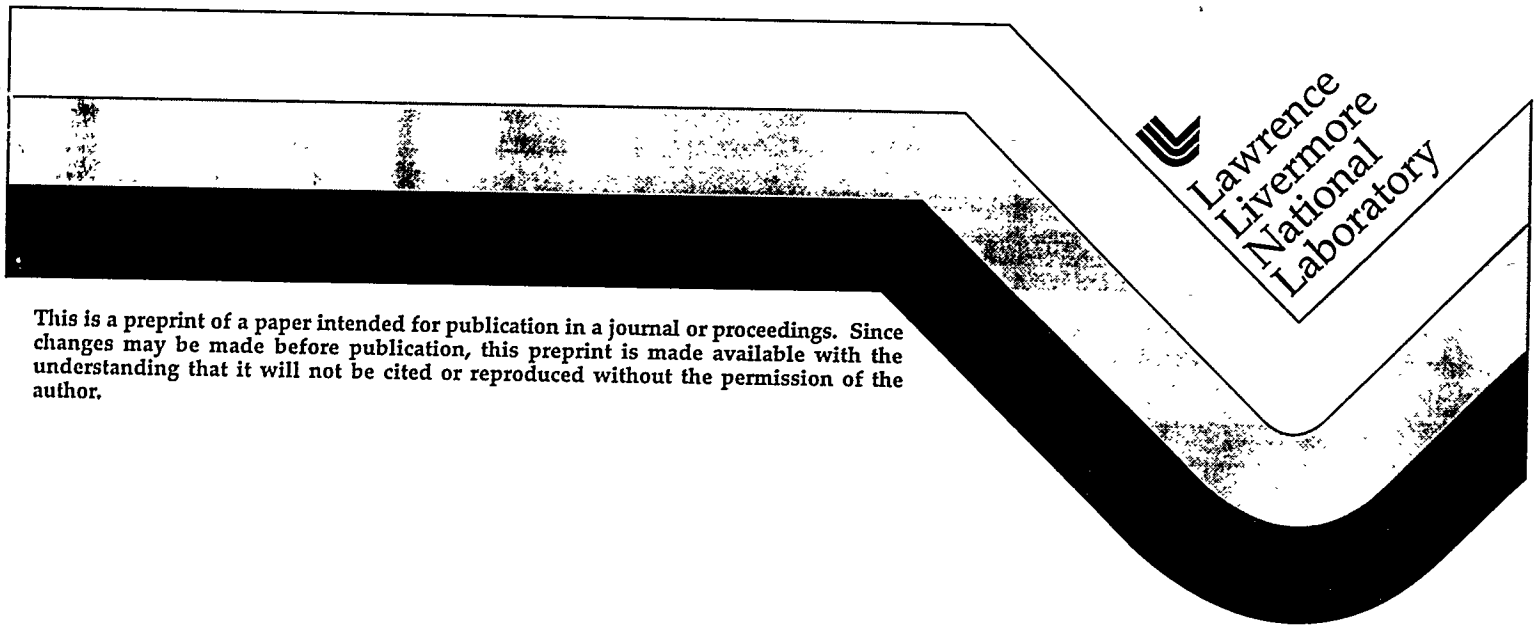

Simulation of experimentally achieved detached plasmas using the UEDGE code

Gary D. Porter, S. Allen, M. Fenstermacher, D. Hill, R. Jong, T. Leonard[1], D. Nilson, M. Rensink, T. Rognlien, G. Smith, and the entire DIII-D team[1]

Lawrence Livermore National Laboratory

P O Box 808, L-637

Livermore, California 94550

Abstract

The introduction of a divertor Thomson scattering system in DIII-D has enabled accurate determination of the plasma properties in the divertor region. We identify two plasma regimes; detached and attached. The electron temperature in the detached regime is about 2 eV, much lower than 5 to 10 eV determined earlier. We show that fluid models of the DIII-D scrape-off layer plasma are able to reproduce many of the features of these two plasma regimes, including the boundaries for transition between them. Detailed comparison between the results obtained from the fluid models and experiment suggest the models underestimate the spatial extent of the low temperature region associated the detached plasma mode. We suggest that atomic physics processes at the low electron temperatures reported here may account for this discrepancy.

---

[1]General Atomics, P O Box 85608, San Diego, CA 92186

I. Introduction

The design of a viable divertor for the International Tokamak Experimental Reactor (ITER) has focused attention on our understanding of the plasma parameters outside the last closed flux surfaces (the Scrape-off Layer, or SOL) of a diverted tokamak device[1,2]. A successful divertor design must not only reduce the power load to a technically manageable value, it must also provide control of sputtering rates, impurity influx to the core plasma, and the influx of hydrogenic neutrals to the core plasma. Concern about the divertor heat loads has led the ITER design team to propose operation with detached plasmas, a SOL plasma operating mode which has been observed in present day tokamaks[3,4,5]. This operating mode is characterized by low power loading at the divertor plate, low ion currents to the plate, and low plate electron temperature. Each of these characteristics make the detached plasma mode very desirable for use in ITER. However, there is not yet enough known about the SOL plasma in this mode to determine its compatibility with other divertor requirements, nor do we adequately understand the compatibility of the detached mode with requirements for the core plasma in ITER. We describe both recent experimental measurements and simulations of detached plasmas in DIII-D in this report.

This paper is organized as follows: we describe recent experimental results, including data from the recently installed divertor Thomson system in Section II. We describe the results of UEDGE simulations of DIII-D in Section III, with both a general description of the calculated SOL plasma modes and a detailed description of code validation efforts. We conclude with a summary in Section IV.

II. Experimental characterization

The DIII-D tokamak has an extensive set of diagnostics for the SOL plasma. It includes a Thomson scattering array at the top of the device from which we obtain a radial profile of the electron density and temperature from near the plasma center to well outside the last close flux surface; a Charge Exchange Recombination (CER) array which provides measurements of the radial profile of the ion temperature from the plasma center through the SOL at the outer mid plane of the plasma; an infra red television (IRTV) system which is used to measure the heating power loads on all surfaces, including the divertor plates; two bolometer arrays which provide poloidal profiles of the total radiated power in the core and SOL plasmas; a Langmuir probe array on the divertor floor which provides measurement of the plasma density and temperature; an insertable Langmuir probe at the outer mid plane; and numerous camera views which permit imaging of the plasma in visible light from specific impurity and hydrogenic species. Additional diagnostics have recently been installed to better understand the behavior of impurities in the divertor region.

In this paper we describe initial results from a new Thomson Scattering system which determines the plasma electron density and temperature in the divertor region of DIII-D[6,7]. This diagnostic permits measurement of the plasma parameters along a vertical line which extends about 21 cm from the divertor floor. There are eight detection channels with a vertical spacing between 1 and 1.5 cm. The laser which is used for this measurement is capable of operation with a pulse rate of 20 Hz, permitting plasma measurements every 50 ms throughout a discharge. We obtain a 2-D profile of the plasma density and temperature by moving the plasma equilibrium radially on a time scale which is slow relative to pulse rate of the laser.

A. Measurement geometry

To fully characterize the divertor plasma near the outer strike point, we must move the plasma equilibrium at least a distance which corresponds to the radial

displacement between the X-point and the outer strike point, a distance of about 0.2 to 0.3 m in DIII-D. Unfortunately, it is not possible to keep the plasma shape constant while sweeping the X-point over such large distances. Hence, it is necessary to cast the measured density and temperature onto a spatial coordinate system which reflects the magnetic geometry. The coordinate system we have chosen is described in Fig. 1. The normalized poloidal flux, Ψ_N, and the poloidal distance along a flux surface to the plate, L_{pol}, is determined for each of the eight measurement locations indicated schematically in Fig. 1. Measurements which lie below the X-point, and have $\Psi_N < 1.0$, lie in the private flux region of the plasma. All data taken at $\Psi_N > 1.0$ lie in the SOL. Data taken above the X-point, with $\Psi_N < 1.0$, lie on closed flux surfaces in the core plasma. Since these flux surfaces do not connect to the divertor plate, we can not define L_{pol}. We do not include these core data in the 2-D plots of the divertor plasma, but restrict the data to the private flux and SOL regions.

B. Experimental results

The experimental results described in this paper have been obtained during recent DIII-D experiments designed to characterize the SOL plasma. The plasma was operated in a lower single null configuration with relatively high triangularity (δ~0.5); moderate plasma current (I_p~1.5 MA); and variable neutral beam heating (2 MW $\leq P_{beam} \leq$ 8 MW). In general, we find the divertor plasma is at, or near, detachment on the inner divertor, and attached at the outer divertor. Although some operation with low beam heating powers produced L-mode (Low confinement) in the core plasma, the data described in this paper is restricted to operation in H-mode (High confinement). The plasma density increased for a few hundred milliseconds after the transition to H-mode, then equilibrated after the onset of Edge Localized Modes (ELMs). The X-point was swept radially during the equilibrium phase of the

plasma. We obtained detachment from both the inner and outer divertors by introducing additional gas (either D_2 or an impurity such as N_2, Ne, or Ar).

The plasma density for an attached divertor plasma is shown together with the density for a detached plasma in Fig. 2. Plasma operation was similar for the two cases shown in this figure except that additional Deuterium gas was introduced to obtain detachment. As can be seen in this figure, the plasma density for the attached case is maximum near the separatrix at the plate, while the maximum density occurs in the SOL away from the separatrix for the detached case. In addition, the plasma density for the detached plasma is about $4 \times 10^{20}\ m^{-3}$, approximately a factor of 7 higher than seen for an attached plasma. The profile of the electron temperature for these two cases is shown in Fig. 3. The electron temperature of the attached plasma falls from a maximum of about 120 eV near the X-point ($\Psi_N = 1.0$; $L_{pol} = 0.28$), to about 15 eV near the separatrix at the plate. On the other hand, the electron temperature for the detached plasma is below 5 eV throughout the divertor region, except near the X-point where the temperature rises to around 10 to 15 eV. It is the difference in the electron temperature at the plate which we use to define the attached and detached plasma modes. The electron temperature in the private flux region ($\Psi_N < 1.0$) is about 2 eV for both detached and attached operation.

These experimental results clearly indicate the existence of at least two SOL plasma modes. One mode, attached plasma, is characterized by high electron temperature at the plate, and the other by very low electron temperatures. Other experimentally observed characteristics of these two modes have been described previously[8]. We explore the physics of these operating modes by examining simulations of the SOL plasma in the next section.

III. Simulation results

The SOL plasmas in DIII-D are simulated using the 2-D fluid plasma code UEDGE[9]. This code solves fluid equations for plasma density, energy, and momentum together with a model for neutral particles. The equations are solved in a flux-based coordinate system to more accurately model the large difference in parallel and perpendicular transport rates. We use a 9-point differencing scheme to permit use of non-orthogonal grids, thus allowing more accurate representation of realistic divertor geometry. Transport parallel to field lines is assumed to be classical with flux limits imposed to correct the classical fluxes for kinetic effects when the collision mean free path is long relative to gradient scale lengths. Transport perpendicular to field lines is assumed to be anomalous, and is modeled by assuming an arbitrary radial diffusion coefficient for particle transport, electron and ion thermal transport, and viscosity transport. Although these diffusion coefficients can be arbitrarily specified, we assume all perpendicular transport coefficients are spatially constant in the results reported here. Neutral particles are treated with an inertial fluid model which allows for parallel momentum exchange between ions and neutrals via charge exchange reactions[10]. We can consider the effect of impurity radiation on the SOL plasma by treating impurities as a separate fluid for each of the ionization states of the assumed impurity[11]. Alternatively, we can assume the impurity density is a fixed fraction of the background plasma. In either case we determine the impurity radiation using an emissivity model which includes enhancements because of charge exchange recombination and finite impurity lifetime[12].

A. Identification of SOL plasma modes

To simulate the DIII-D SOL plasma we start with a plasma shape obtained from magnetic analysis of a specific discharge. Our simulation is intended to be applicable over a narrow region at the edge of this plasma. We start from a closed flux surface inside the separatrix, typically the 98% flux surface, and extend to the first poloidal

flux surface which intersects a material wall, typically in the range $1.05 \leq \Psi_N \leq 1.15$. We specify the power across the inner flux surface, P_{sep}, and the density on that surface, n_{core}, as core boundary conditions. The radial power flow is distributed poloidally to provide approximately constant density and temperature on the innermost flux surface, as expected because of high parallel conductivity. This means that the majority of the radial power is transported at the outer mid plane where the flux surfaces are maximally compressed. The perpendicular particle diffusion coefficient, and electron and ion thermal diffusivities are determined empirically by matching the upstream density and temperature radial profiles measured in DIII-D. We used values of $D_\perp = 0.3\ m^2/s$, $\chi_e = \chi_i = 1.5\ m^2/s$ for the simulations reported in this section. We determine the existence of multiple SOL plasma modes by examining the dependence of the plasma parameters on the separatrix density and power. The results are summarized in Fig. 4, and the variation of the plate electron temperature at the separatrix with heating power and core density is shown in Fig. 5. The parameters for which we have converged UEDGE solutions are indicated by the circles, squares, and diamonds on Fig. 4.

When the core plasma density is low, and/or the separatrix heating power is high, we find the separatrix temperature to be high at both the inside and outside divertor plates–characteristic of attached plasmas. When the heating power is reduced, at fixed core density, the plate electron temperature decreases. Since the connection length from the outer mid plane to the inner divertor plate is longer than that to the outer divertor plate, we find the inner electron temperature decreases more rapidly than the outer. The temperature drops more rapidly with decreasing power when it falls below that necessary for efficient ionization of neutrals, about 10 eV. We somewhat arbitrarily define the transition from attached to detached plasmas as being the power at which the plate temperature drops below 5 eV. At these low

temperatures, the neutral gas which originates from recycling of ions on the plate is no longer efficiently ionized. Rather, the gas can escape from the region of maximum ion current density (near the separatrix) and be pumped on the walls before being ionized. This leads to a decrease in the ion current reaching the plate, as seen in experiment. Since the electron temperature decreases more rapidly on the inner plate, we find detached operation on the inside first. When the power is decreased further, the plasma also detaches at the outer plate. This inside/outside asymmetry is also observed in experiment. When the power is reduced below that required to detach at both the inner and outer plate, the plasma region with reduced electron temperature moves up off the plate toward the X-point. Finally, when the 5 eV electron temperature contour reaches the X-point neutral gas can penetrate to the core plasma and we find a third plasma mode, the core MARFE. In this case we obtain a local maximum of the plasma density on the closed flux surfaces, just above the X-point.

The UEDGE simulations used to obtain the results shown in Figs. 4 and 5 were done for pure hydrogen plasmas, i.e. without impurities. The power lost by radiation in the SOL arises from radiation associated with ionization of the recycling neutrals in this case. Typically the power radiated is on the order of 10 to 20% of the power across the separatrix for attached solutions, and increases to 40 to 50% just before the transition to the core MARFE. The radiated powers are relatively unimportant in the region which defines the transition from attached to detached plasma modes. We have also run UEDGE simulations in which both the core density and the separatrix power are kept constant, and the SOL radiation power is varied by varying an impurity concentration. As expected, we find that the plate electron temperatures decrease as the impurity radiation power is increased by raising the impurity concentration. Indeed, the temperature at the inner plate decreases very rapidly

since the inner plate density is quite high, leading to very high radiated powers near the inner plate. Hence we found the transition to the detached state behaves similarly to that shown in Fig. 4. These results indicate that the critical parameter for determination of the detachment threshold is the power delivered to the divertor plate, and hence the power which is available for re ionization of recycling neutrals. Earlier simulations have shown that similar effects can be achieved by injecting neutral gas into the SOL. Hence we find that the code simulations mirror experiment in that we can induce detachment by injecting gas or impurities into the SOL.

An issue which is of some interest to ITER is the poloidal variation of the plasma pressure. When the plasma is operated in a regime in which the parallel power flow is limited by sheath effects, the power density to the plate can be approximated by the following equation.

$$P_{plate} = k_1 [n_e T_e] \cdot \sqrt{T_e} + 13.6\, J_{ion}$$

Where the second term is the power associated with recombination of the ion current to the plate, J_{ion}. If the plasma pressure does not vary poloidally, as one would expect if there were no mechanisms for momentum removal, enhanced radiation effects can only reduce the power to the plate by reducing the plate temperature, and the power is only reduced as the square root of the temperature. As we showed in Section 2, we observe roughly an order of magnitude drop in divertor temperature at the transition to detachment, hence one would expect about a factor of 3 decrease in divertor heating power. The power density will be reduced somewhat more than this because of the reduction in the plate ion current associated with the detached mode, and the concomitant reduction in the power associated with recombination of that current. Design studies for the ITER divertor suggest the

plate power must be decreased by something like an order of magnitude, hence there must be a mechanism for momentum removal from the plasma, and a concomitant poloidal decrease in plasma pressure. Several possible mechanisms for momentum removal exist including radial transport of viscosity and charge exchange reactions between ions and neutrals. If the electron temperature of the detached state is below 5 to 10 eV, as indicated in both the DIII-D experiment and the UEDGE simulations described above, one expects charge exchange reactions to dominate and provide a mechanism for momentum removal. We show the poloidal variation of the total plasma pressure (thé sum of the electron pressure, the ion pressure, and the kinetic pressure associated with plasma flow) for two different heating powers at a fixed core density in Fig. 6. At a high power, the plasma pressure is essentially constant poloidally, even though the inner divertor has become detached. As the power is decreased, the region of low electron temperature increases, and momentum removal by both radial transport of viscosity and charge exchange reactions become more important. At the lowest power achieved before the transition to the core MARFE regime, we find a decrease in the total plasma pressure on the order of a factor of 2 to 3. All of this pressure drop occurs below the X-point at both the inner and outer divertor plates.

We have shown in this section that the fluid simulations of the DIII-D plasmas successfully reproduce many of the features of the SOL plasma which are seen in the experiment. The question of the value of these code for detailed design of future devices such as the ITER divertor then naturally arises. To address this question we must first make a detailed comparison of code simulations with experimental results. We will do this in the next section.

B. Detailed code validation results

We have chosen a discharge without gas or impurity puffing for detailed comparison with numerical simulation. This discharge, shot 86586, had approximately 6.7 MW of neutral beam heating into a lower single null plasma configuration with 1.4 MA of plasma current. Analysis of the power flow for this discharge shows that approximately 6.4 MW is flowing into the SOL; approximately 2.5 MW is radiated in the SOL, and 3.5 MW is observed as heating of the divertor plates (0.4 MW of SOL heating power is not accounted for experimentally). The position of the X-point was moved radially approximately 0.2 m during this discharge, permitting determination of the 2-D profile of divertor density and temperature. The result has been shown as the attached case in Figs. 2 and 3. At 2550 ms, the time chosen for detailed comparison, the plasma is positioned so that the divertor Thomson system obtains data from both the private flux region and the SOL. The core plasma is in an ELMing H-mode phase at this time. We make no attempt to simulate the effect of ELMs in this paper, so we have simply averaged the experimental data over several ELMs to obtain time-averaged plasma parameters.

The UEDGE simulation of this discharge is done by using the total power into the SOL as a boundary condition at the innermost flux surface, the 98% poloidal flux surface. We assume the power is evenly split between flow in the electrons and ions. We use spatially constant perpendicular transport coefficients, and adjust them to obtain consistency between the simulated and experimental radial profiles of the upstream density and temperature. The calculated radial profiles of density and temperature are shown as a function of radial displacement from the separatrix at the outer mid plane, together with the experimentally measured profiles in Fig. 7. The diffusion coefficients used to obtain these profiles were $D_\perp = 0.3\ m^2/s$; $\chi_i = \chi_e = 1.5\ m^2/s$. Note that experimental data for the ion temperature in the SOL does not exist for the particular discharge chosen here. This means we do not have a

believable estimate for the ion thermal diffusivity since we would have to compare with details of the ion temperature profile. We have chosen to make the ion and electron diffusivities equal for simplicity. Ion temperature measurements obtained on similar discharges indicate that the high, broad profile obtained in the simulation is qualitatively consistent with experiment.

Having obtained reasonable consistency with the upstream density and temperature profiles, we must now compare with other measurements of the SOL plasma parameters. In particular, we want to compare the simulation with measurements in the divertor region. Two other input parameters can affect the UEDGE simulation in this region; the assumption for the neutral recycling coefficient at the plate, and assumptions for impurities. Ion fluxes to the divertor plates are very large. Hence we expect the carbon of the divertor to become saturated with deuterium very early in the discharge. If so, one would expect a plate recycling coefficient of unity, i.e. a neutral atom off the plate for every ion into the plate. We have made this assumption in our simulations. We use the experimentally determined power radiated in the SOL as a guide for impurities in our simulation. Specifically, we have used a simple fixed impurity concentration, and adjusted the concentration to obtain a total radiated power consistent with the experiment. We find a Carbon impurity fraction of 0.65% is required to obtain a total radiated power of 2.5 MW, as measured experimentally. Approximately two-thirds of the power is radiated by impurities, the remaining one-third is radiated by deuterium due to re ionization of the recycled neutrals. We compare the simulated divertor density and temperature profile with that measured by the divertor Thomson system in Fig. 8. The abscissa of this figure is measurement of the vertical coordinate in DIII-D; the divertor floor lies at 0.235 m in this coordinate, and the separatrix position for the radial position of the divertor Thomson (R=1.493 m) is at 0.29 m. As can be seen in Fig. 8, the UEDGE simulation

agrees quite well with experiment in the private flux region, although the simulated electron temperature is slightly higher. The simulated electron temperature in the SOL is in reasonable agreement with experiment, although the simulated density is significantly higher than experiment. This discrepancy is the first indication that the simulation does not quite have the physics of neutral recycling correct.

We compare with other measurements at the divertor to obtain more complete understanding of this discrepancy. In particular we want to compare with measurements of the divertor heat flux, and of the H_α emission associated with re ionization of neutrals at the divertor. The simulated peak divertor heat agrees quite well with that measured by the IRTV system, both at the outside and the inside strike points. The peak heat flux on the inside is about a factor of three lower than that on the outside, in both the experiment and the simulation. However, the simulation indicates a narrow peak at the separatrix with a broader, lower level heating extending radially into the SOL. The simulation underestimates the heat flux by about a factor of two in the broad region. The discrepancy of the simulated H_α emission is of greater interest since it provides guidance for improvement in the theoretical model. The H_α emission is measured by an absolutely calibrated seven channel photo diode array which views the divertor floor from the top of the tokamak. Each channel is collimated to view a 5 to 10 cm diameter region of the floor. We compare the simulation of this measurement to the experiment in Fig. 9. The simulation is consistent with experiment near both the inner and outer strike points (R = 1.14 m and R = 1.54 m respectively). Both the simulation and experiment indicate the emission is higher away from the separatrix on the inside, suggesting that the neutral density is relatively high over a broad radial range about the inner strike point. However, the simulation underestimates the H_α emission for the three photo diodes which view the floor in the private flux region by at least an order of

magnitude. This discrepancy suggests that we are seriously underestimating the flow of neutrals to the private flux region; most probably having originated from recycling at the inner strike point. Note that if there were higher neutral densities in the private flux region, there would also be larger radiation losses along the separatrix on the outer divertor leg. This would probably reduce the high electron temperature at the outer separatrix, and hence the local high divertor power flux. This would improve the agreement between simulation and experiment even further.

We can gain some insight about the origins of the discrepancy in H_α emission by examining the profile of the electron temperature in the divertor region. We show the simulated electron temperature profile over the entire divertor region, together with the experimental and simulated 2-D profile of the outer separatrix region as measured on the divertor Thomson system, in Fig. 10. The simulation indicates the electron temperature at the inner plate has collapsed, the temperature on the plate is in the 1 to 2 eV range, leading to the low divertor power seen in both the experiment and simulation. However, the region of low electron temperature does not extend very far toward the X-point; the 5 eV contour lies only about 1 cm off the plate. This means that neutrals which recycle from near the separatrix on the inner plate have a high probability of being reionized before escaping to a wall and being pumped. Neutrals which flow toward the SOL from the inner strike point encounter a region with low electron temperature, hence the ionization mean free path is fairly long. This leads to the high H_α emission which is seen in both the experiment and simulation at R = 1.06 m. However neutrals which flow toward the private flux region are rapidly pumped by the plasma along the separatrix and flow back to the strike point. One would expect a higher neutral density in the private flux region, and hence a higher H_α emission, if the 5 eV contour lay further up the separatrix on

the inner divertor leg. This suggests we must examine the model used for the low temperature region to better simulate the experiment.

IV. Conclusions

We have shown exciting new measurements of the plasma density and temperature in the divertor region of DIII-D. These data have been obtained using a newly installed divertor Thomson scattering system. We have demonstrated clear evidence of the existence of two plasma regimes for the SOL, detached and attached. Attached plasmas are characterized by high temperature ($T_e \geq 10$ eV) at the divertor plate and relatively low density. On the other hand, the plate density is a factor of 7 higher for the detached plasma state, and the electron temperature is 2 eV.

We also observe the existence of two plasma regimes in simulation of the DIII-D SOL plasma using the UEDGE. We find the detached regime is obtained first at the inner divertor plate then, at lower power, at the outer leg. This is similar to behavior seen in experiments. The powers at which we achieve detachment in our simulations are comparable to those found experimentally. The detached state can be achieved by reducing power; increasing plasma density; gas puffing; and impurity injection in both simulation and experiment. Our simulations indicate the region of low electron temperature expands up the separatrix toward the X-point as the power is reduced below that required to achieve detachment. When the low temperature region expands far enough to permit neutral penetration to the closed flux surfaces, we obtain a localized high density region on the closed flux surfaces, similar to MARFEs seen experimentally. These similarities between experiment and simulation are very encouraging about our ability to apply the SOL plasma models to the design of divertors for future devices such as ITER.

We have shown detailed comparisons between simulation and experiment for a particular DIII-D discharge. While we have accurately reproduced many of the experimental results, we find an important discrepancy in the simulation of H_α emission from neutrals which recycle at the divertor plate. One interpretation of this discrepancy is that the low temperature region which is associated with the detached plasma state is larger in the experiment than predicted by the model. This, in turn, suggests that our models do not adequately reflect the physics of this low temperature region. The new experimental results indicate the temperature in the region is in the range of 1 to 2 eV rather than 5 to 10 eV indicated in earlier results. It has been suggested by Post[12] that there are many important atomic physics processes exist when the electron temperature is this low. These processes are not in the current models. It is hoped that the computer models described in this report will accurately reproduce both the attached and detached plasma states when these processes are introduced.

Acknowledgment

We happily acknowledge many valuable discussions with R.D. Stambaugh and A. Mahdavi about the work described in this report. This work was supported under U.S. DOE auspices by Lawrence Livermore National Laboratory, contract No.W-7405-ENG-48, and General Atomics, contract No. DE-AC03-89ER51114.

References

1 Post's IAEA paper

2 G. Janeschitz, K. Borrass, G. Federici, Y. Igitkhanov, A. Kukushkin, H.D. Pacher, G.W. Pacher, M. Sugihara, "The ITER divertor concept", J. Nucl. Mat., 220-222, p. 73-88, 1995.

3 T. W. Petrie, et.al., "Radiative Divertor Experiments in DIII–D with Deuterium Injection", submitted to Nucl. Fus., 1995.

4 B. Lipschultz, J.A. Goetz, I.H. Hutchinson, B. LaBombard, G.M. McCracken, A. Niemszewski, J.L. Terry, S.M. Wolfe, "An Investigation of the Extent of Divertor Detachment in Alcator C-Mod", 22nd European Physical Society Conference on Controlled Fusion and Plasma Physics, p III-325, July, 1995.

5 G.F. Matthews, D.J. Campbell, S. Clement, S.J. Davies, J. Ehrenberg, I. Garcia-Cortes, H.Y. Guo, P.J. Harbour, H. Jackel, A. Loarte, C. Lowry, J. Lingertat, R.D. Monk, D.P. O'Brien, R. Reichle, G. Saibene, M.F. Stamp, A. Taroni, R. Simonini, G. C. Vlases, M.G. Von Hellermann, "Highly Radiating and Detached Divertor Plasmas with Carbon and Beryllium Targets", 22nd European Physical Society Conference on Controlled Fusion and Plasma Physics, July, 1995.

6 T.N. Carlstrom, et al., Rev. Sci. Instrum. 66 (1995), p495.

7 D. G. Nilson, T. N. Carlstrom, et al., "Initial Operations of the Divertor Thomson Scattering Diagnostic on DIII-D", to be submitted to Rev. Sci. Instrum.

8 G. Matthews, "Plasma detachment from divertor targets and limiters", J. Nucl. Mat., **220-222**, p. 104-116, (1995).

9 T. Rognlien, J.L. Milovich, M.E. Rensink, G.D. Porter"A fully implicit, time dependent 2-D fluid code for modeling tokamak edge plasmas", J. Nucl. Mat., **196-198**, p. 347-351, (1992).

10 F. Wising, S.I. Krasheninnikov, D.J. Sigmar, D.A. Knoll, and T.D. Rognlien, "Simulation of divertor detachment in ITER using the UEDGE code and an advanced neutral model", Bull. Am. Phys. Soc., **40**, 1879 (1995).

11 S.P. Hirshman, and D.J. Sigmar, "Neoclassical transport of impurities in tokamak plasmas", Nucl. Fus., **21**, 1079 (1981).

12 D.E. Post, "A review of recent developments in atomic processes for divertors and edge plasmas", J. Nucl. Mat., **220-222**, p. 143-157, (1995).

Figure Captions

Figure 1 The definition of the geometry which is used to display the 2-D profiles of electron density and temperature obtained from the divertor Thomson scattering system in DIII-D.

Figure 2 The experimentally measured plasma density near the outer strike point for an attached (left) and detached (right) plasma.

Figure 3 The experimentally measured plasma electron temperature near the outer strike point for an attached (left) and detached (right) plasma.

Figure 4 The boundaries for divertor operation in the attached and detached plasma modes. The boundaries are obtained by simulation of the DIII-D tokamak. The parameter n_{core} is the plasma density at the 98% flux surface, and the parameter P_{sep} is the power across the same flux surface.

Figure 5 The behavior of the electron temperature at the separatrix on the inner (top) and outer (bottom) strike points as a function of SOL heating power and upstream plasma density. The detached state is defined as the point at which the temperature at the separatrix drops below 5 eV.

Figure 6 Poloidal variation of the plasma pressure for two values of separatrix heating power at a fixed core density of $0.27 \times 10^{20}\ m^{-3}$. This variation is determined using the UEDGE code with a typical DIII-D plasma configuration.

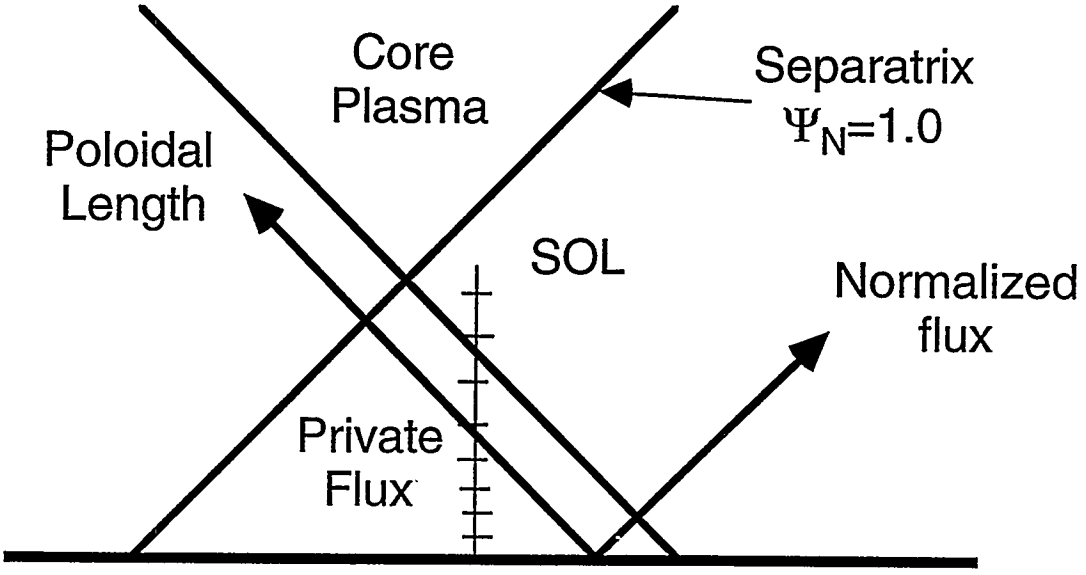
Core
Plasma
Separatrix
Ψ_N=1.0
Poloidal
Length
SOL
Normalized
flux
Private
Flux

Figure 1

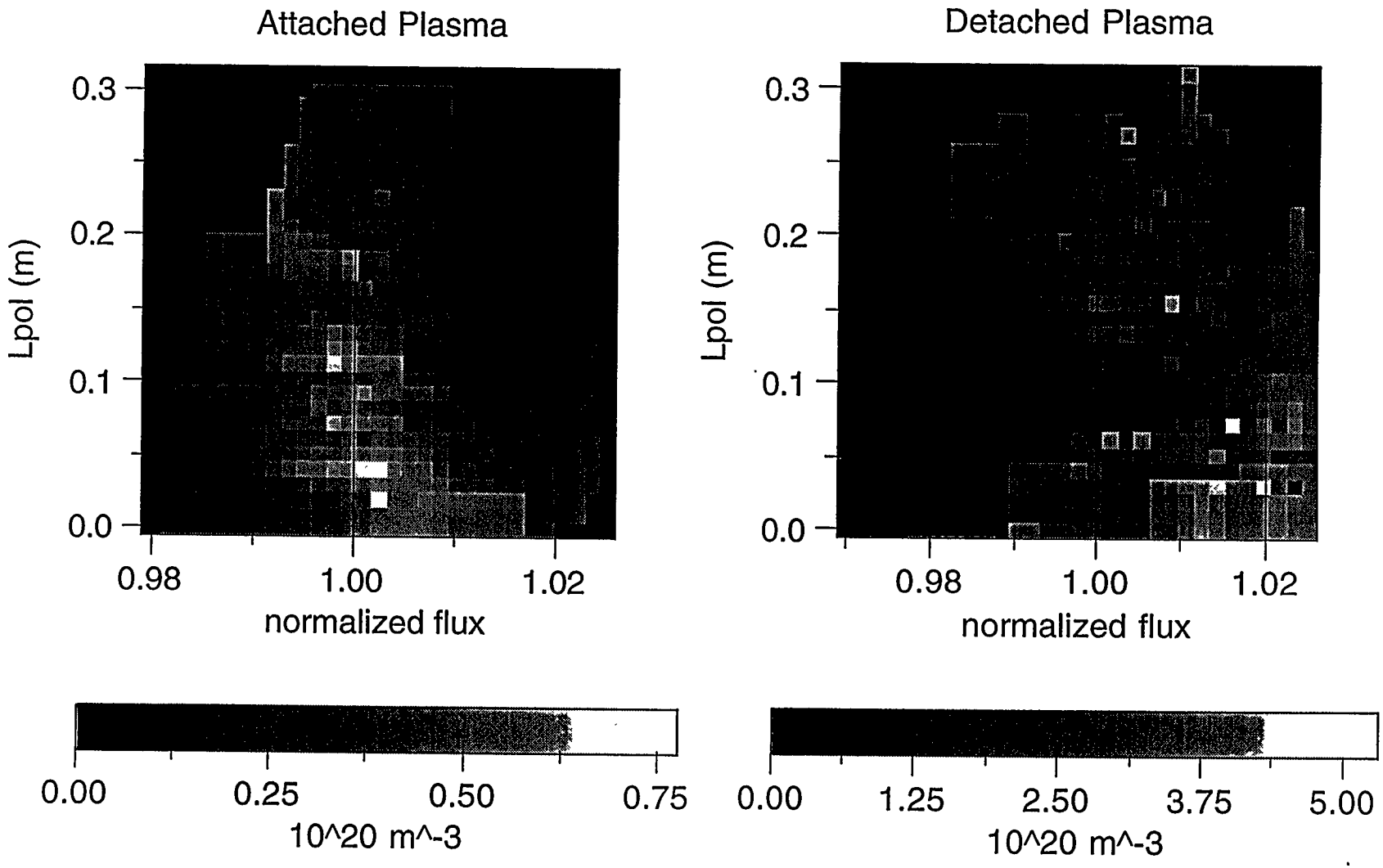
Attached Plasma
Detached Plasma
Lpol (m)
0.3
0.2
0.1
0.0
0.98
1.00
1.02
normalized flux
0.00
0.25
0.50
0.75
10^20 m^-3
1.25
2.50
3.75
5.00

Figure 2

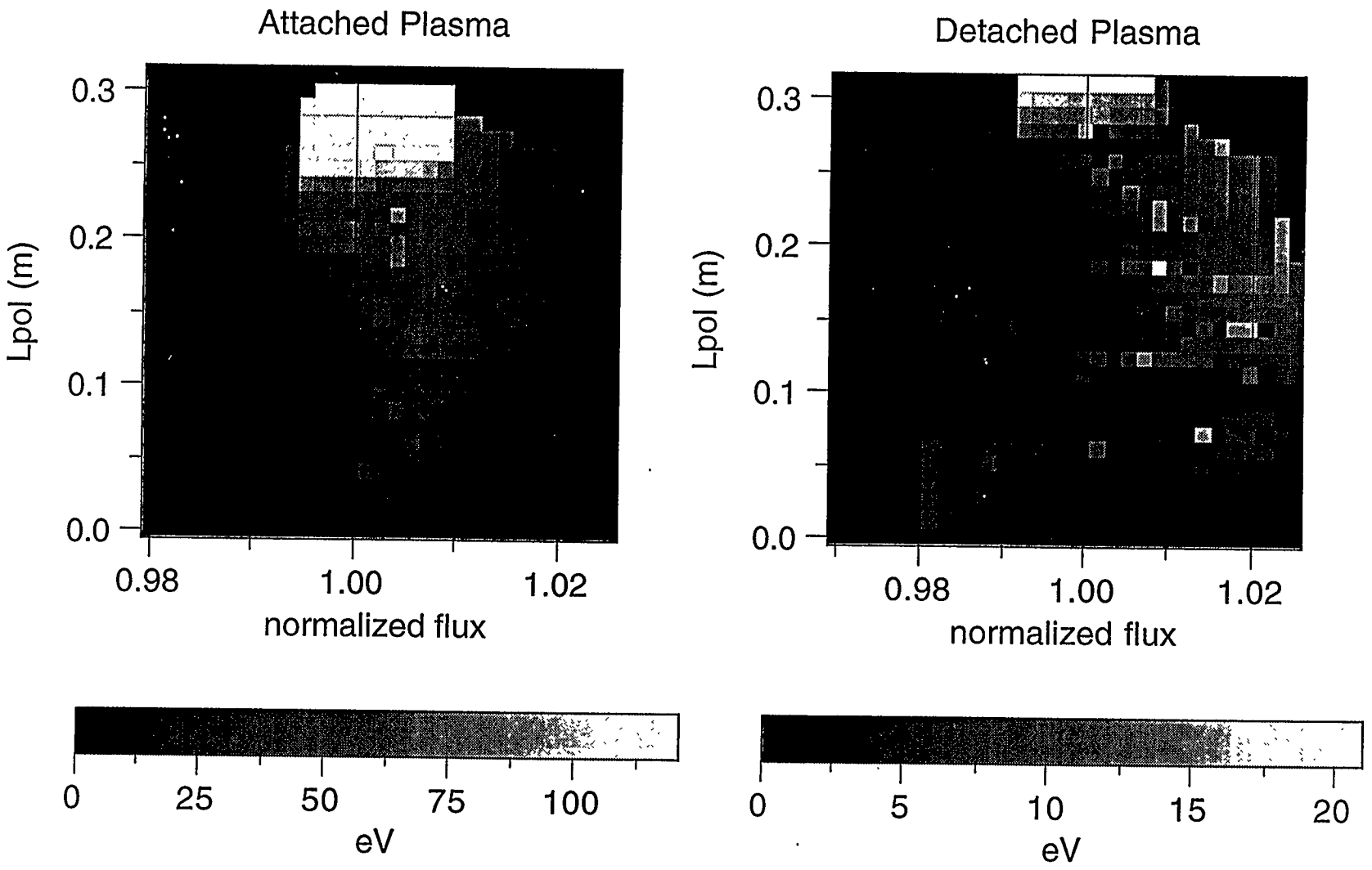
Attached Plasma
Detached Plasma
Lpol (m)
0.3
0.2
0.1
0.0
0.98
1.00
1.02
normalized flux
0
25
50
75
100
eV
0
5
10
15
20
eV

Figure 3

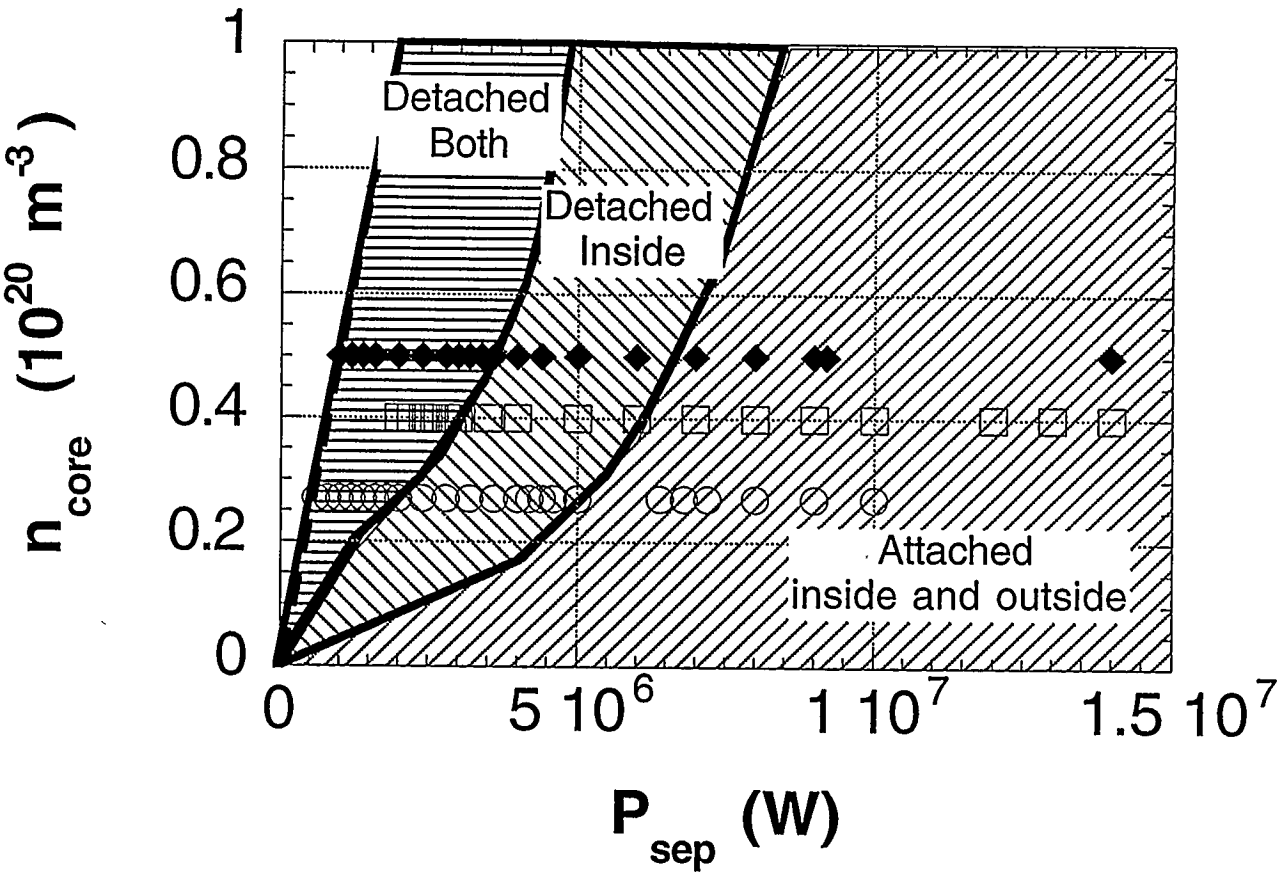
Detached
Both
Detached
Inside
Attached
inside and outside
1
0.8
0.6
0.4
0.2
0
0
5 10^6
1 10^7
1.5 10^7
n_core (10^20 m^-3)
P_sep (W)

Figure 4

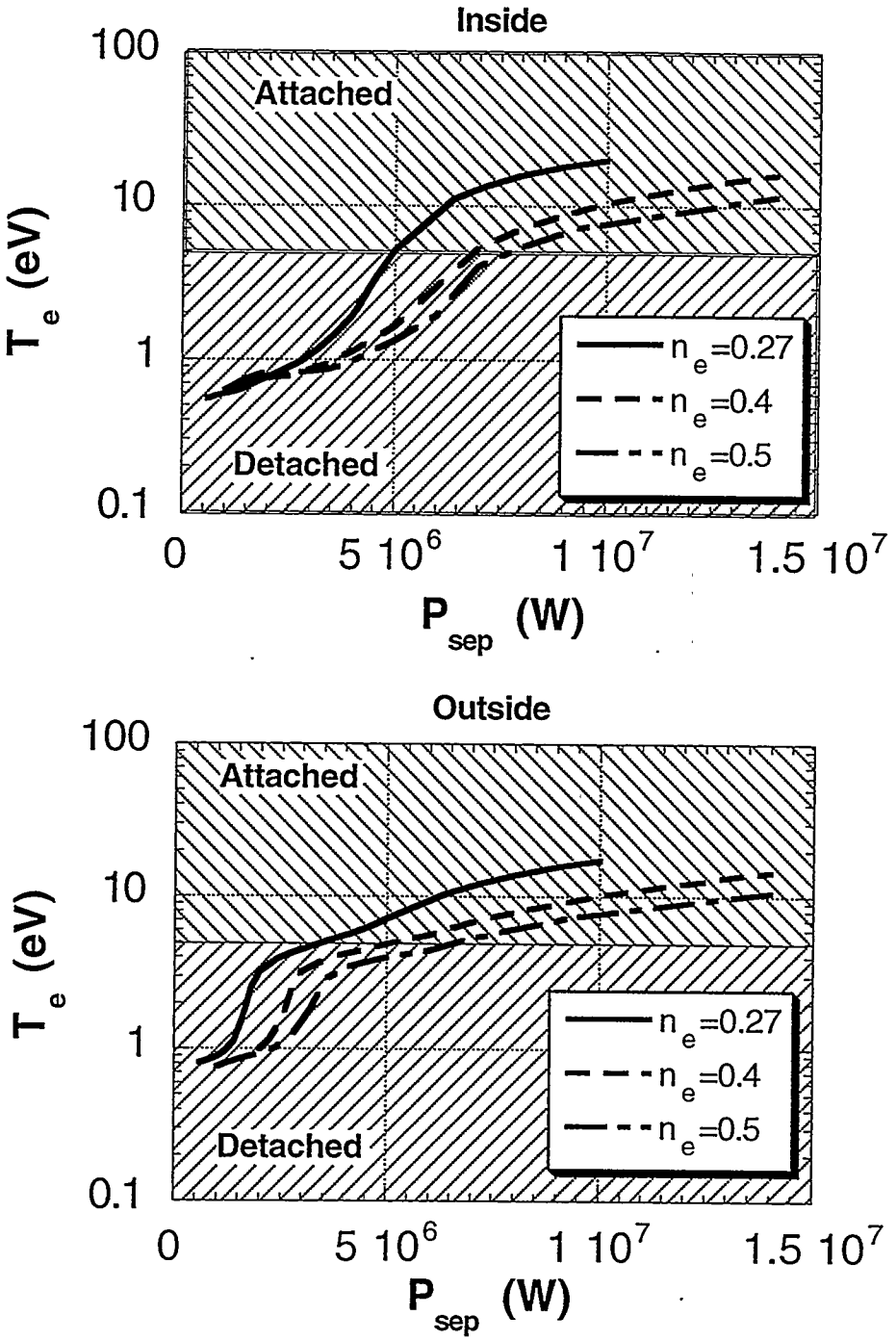
Inside
100
10
1
0.1
Attached
Detached
T_e (eV)
n_e=0.27
n_e=0.4
n_e=0.5
0
5 10^6
1 10^7
1.5 10^7
P_{sep} (W)
Outside
100
10
1
0.1
Attached
Detached
T_e (eV)
n_e=0.27
n_e=0.4
n_e=0.5
0
5 10^6
1 10^7
1.5 10^7
P_{sep} (W)

Figure 5

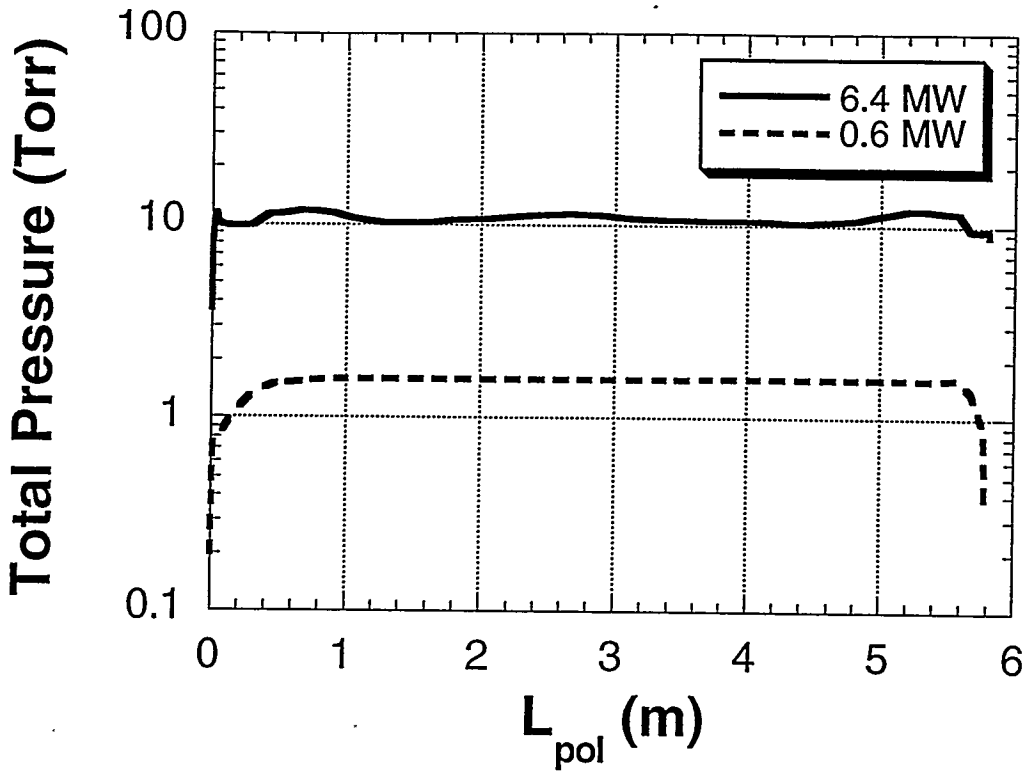

Figure 6

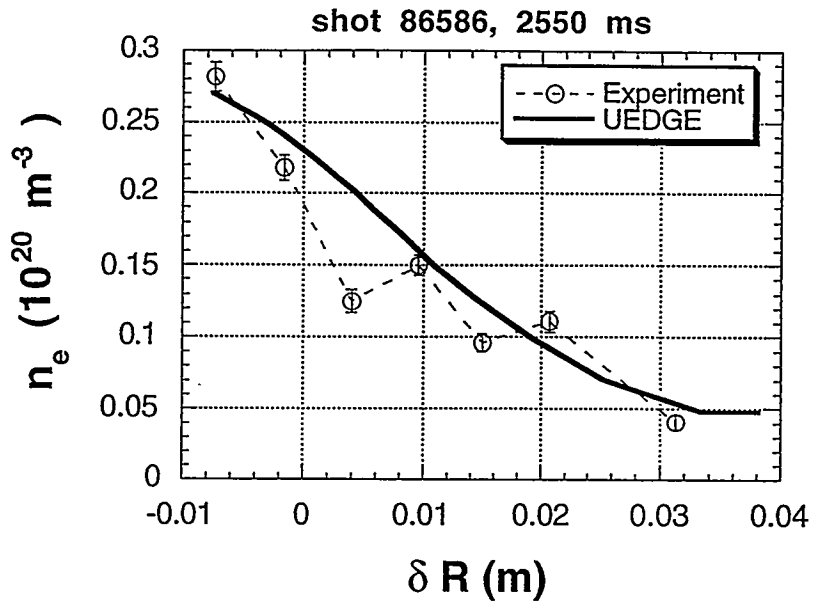
shot 86586, 2550 ms
Experiment
UEDGE
n_e (10^{20} m^{-3})
0.3
0.25
0.2
0.15
0.1
0.05
0
-0.01
0
0.01
0.02
0.03
0.04
δ R (m)

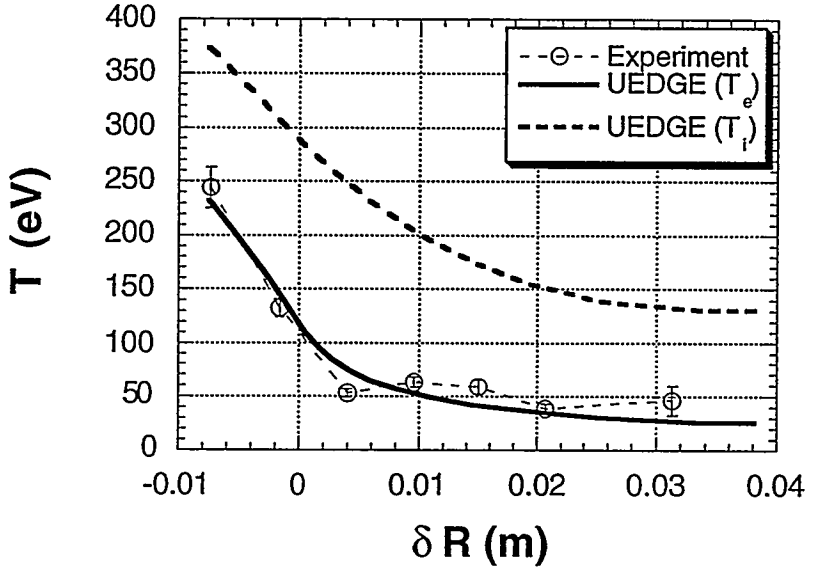
Experiment
UEDGE (T_e)
UEDGE (T_i)
T (eV)
400
350
300
250
200
150
100
50
0
-0.01
0
0.01
0.02
0.03
0.04
δ R (m)

Figure 7

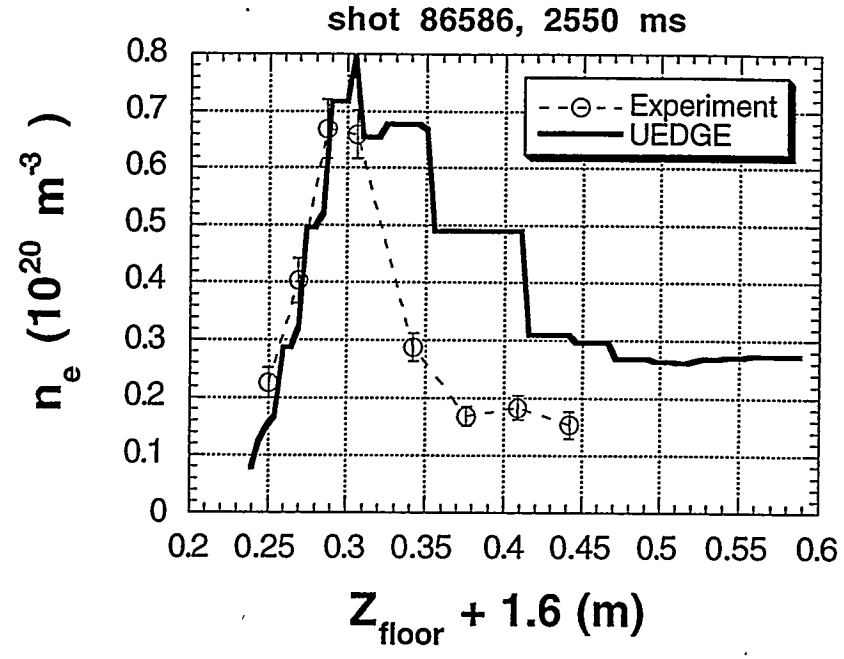
shot 86586, 2550 ms
Experiment
UEDGE
n_e (10^{20} m^{-3})
Z_{floor} + 1.6 (m)

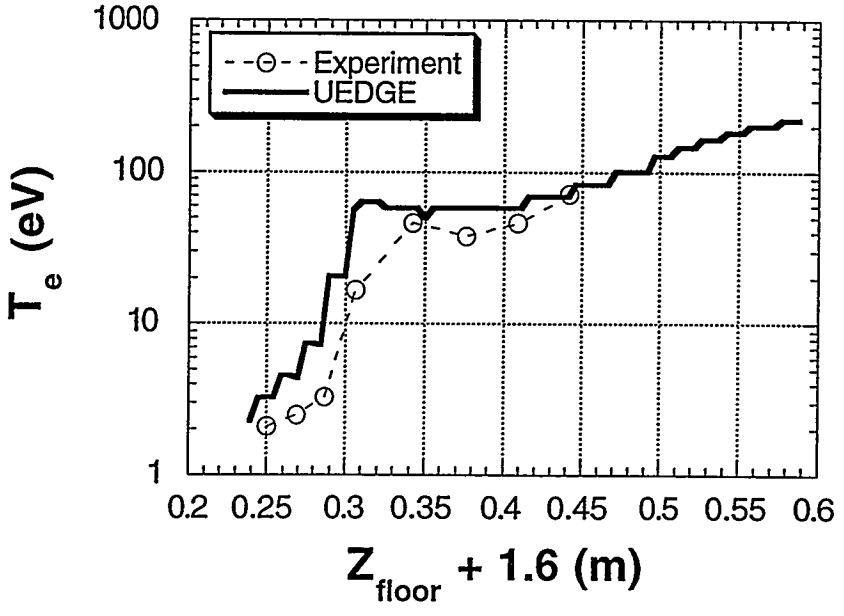
Experiment
UEDGE
T_e (eV)
Z_{floor} + 1.6 (m)

Figure 8

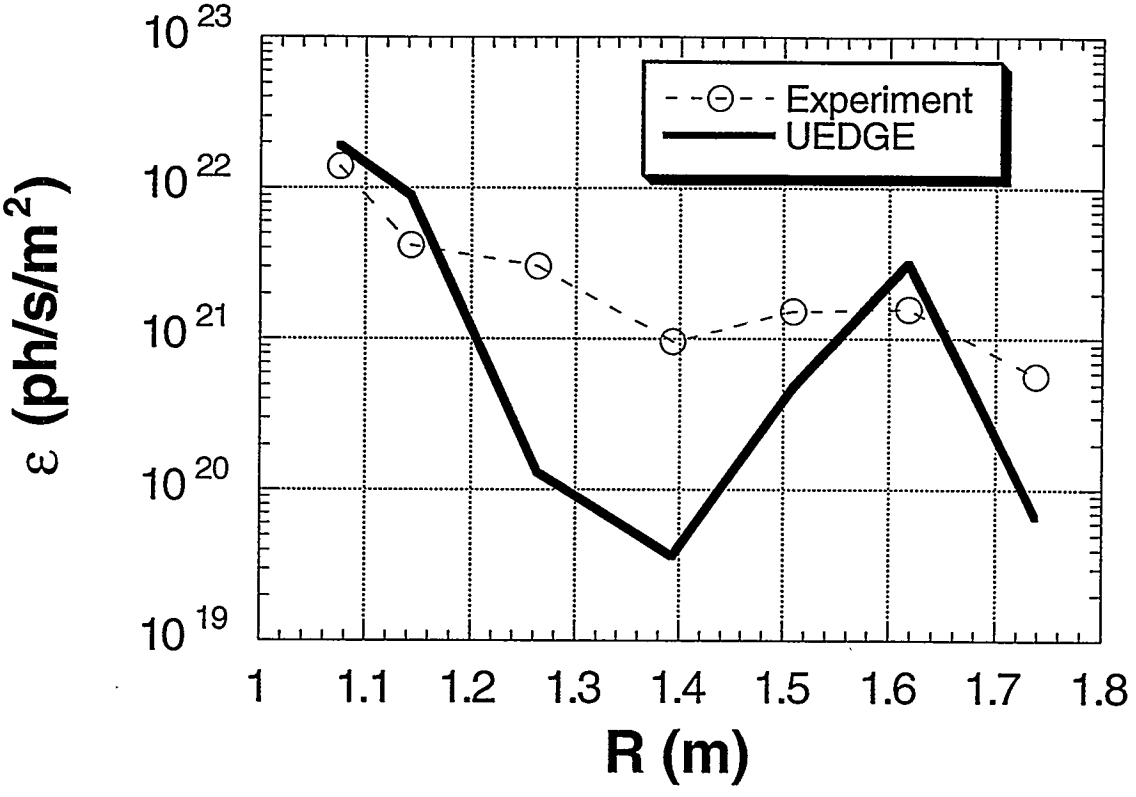
Experiment
UEDGE
ε (ph/s/m²)
10 23
10 22
10 21
10 20
10 19
1
1.1
1.2
1.3
1.4
1.5
1.6
1.7
1.8
R (m)

Figure 9

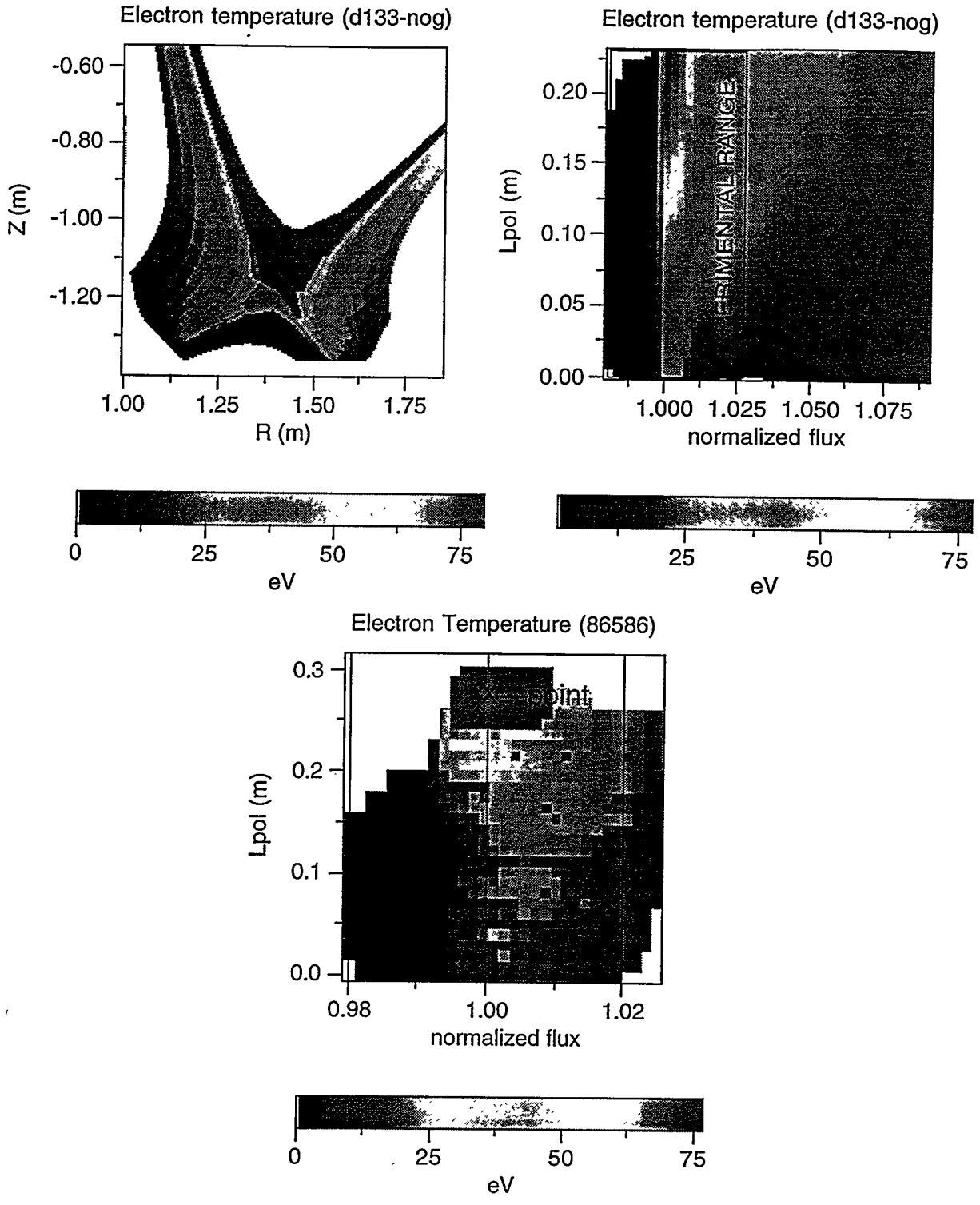
Electron temperature (d133-nog)
-0.60
-0.80
-1.00
-1.20
Z (m)
1.00
1.25
1.50
1.75
R (m)
0
25
50
75
eV
Electron temperature (d133-nog)
0.20
0.15
0.10
0.05
0.00
Lpol (m)
EXPERIMENTAL RANGE
1.000
1.025
1.050
1.075
normalized flux
25
50
75
eV
Electron Temperature (86586)
0.3
0.2
0.1
0.0
Lpol (m)
0.98
1.00
1.02
normalized flux
0
25
50
75
eV

Figure 10